12-13-2003

Applicability of Semi-Tension Fields to the Back Panel of a Pick-Up Truck

Shubha S. Tangirala

APPLICABILITY OF SEMI-TENSION FIELDS TO THE BACK PANEL OF A PICK-UP TRUCK

By

Shubha S. Tangirala

A Thesis
Submitted to the Faculty of
Mississippi State University
in Partial Fulfillment of the Requirements
for the Degree of Master of Science
in Mechanical Engineering
in the Department of Mechanical Engineering

Mississippi State, Mississippi

December 2003

APPLICABILITY OF SEMI-TENSION FIELDS TO THE BACK PANEL OF A PICK-UP TRUCK

By

Shubha S. Tangirala

Approved:

Richard Patton Assistant Professor Mechanical Engineering Department (Director of Thesis)	William Jones Professor Emeritus Mechanical Engineering Department (Committee Member)
John T. Berry Professor Mechanical Engineering Department (Committee Member)	Rogelio Luck Associate Professor Mechanical Engineering Department (Graduate Coordinator)

A. Wayne Bennett
Dean of the College of Engineering

Name: Shubha S. Tangirala

Date of Degree: December 13, 2003

Institution: Mississippi State University

Major Field: Mechanical Engineering

Major Professor: Dr. Richard Patton

Title of Study: APPLICABILITY OF SEMI-TENSION FIELDS TO THE BACK PANEL OF A PICK-UP TRUCK

Pages in Study: 59

Candidate for Degree of Master of Science

The study and design of light-weight automobiles has emerged as an important area of interest in the government, academia, and the manufacturing industry. Significant advances in vehicle weight reduction technologies have taken place in almost all fields of transportation. Weight reduction is identified as a key factor to achieving fuel-economy, energy efficiency and environmental safety.

The main objective of this thesis is to investigate cost effective design methodologies that enable fabrication of light weight structures, which subsequently result in a fuel saving. A few important techniques and trends of weight reduction in the automotive industry over the past few years are studied as part of the thesis. A summary from the survey of various approaches to weight reduction is presented in the literature review.

This thesis is based on the theory of semi-tension fields, which was originally applied towards the design of structures in the aircraft industry. A semi-tension field is a

post buckling phenomenon in which the load is continued to be carried even after the web has buckled. The advantage of semi-tension fields is two-fold: first, by using this theory the structural stability of the original structure is retained; and secondly, its application replaces a comparatively heavy-weight shear resistant web with a thin web, potentially resulting in reduced weight.

The semi-tension field theory is applied to the redesign of back panel of a prototype pick up truck, which was modeled and analyzed using IDEAS Master Series 8 FEA software.

The literature review also consists of the survey of several advances in the Semi-tension fields theory, and the corresponding trends in weight reduction. Analytical theories related to semi-tension field-based design and the respective mathematical formulations have also been described. Finite element analyses of the design that resulted from the application of the theory were carried out and results were validated using analytical theories. A technical paper demonstrating the redesign of a door beam was also studied and results are presented as an appendix.

ACKNOWLEDGMENTS

The author wishes to express her gratitude towards Dr. Richard Patton, her major professor, for his continued support and encouragement through out this thesis. The author would like to thank the Ford Motor Company for funding this research. The author expresses her sincere thanks to her committee members Dr. John Berry and Dr. William Jones for their support during this work. The author would also like to thank Dr.Edward Allen from the Computer Science Department for providing the LaTeX 2_ε template for thesis, which made the typsetting much easier.

TABLE OF CONTENTS

LIST OF TABLES

TABLE Page

LIST OF FIGURES

CHAPTER I

INTRODUCTION

1.1 Background

In recent years importance of the design and development of lightweight vehicles has grown tremendously. Lightweight vehicles are considered a top priority in perspective of several factors related to automotive functionality, fuel-efficiency, economy, and also because of stricter regulations imposed by the government under various environmental safety and energy efficiency programs.

The primary factors motivating continued research and development of light weight automotive structures, as well as materials can be summarized as follows.

- Fuel-economy: "75% of vehicle gas consumption is directly related to factors associated with vehicle weight" [9]. Reducing the vehicle weight results in smaller body parts, including the engines and energy storage systems, contributing to the corresponding cost and/or performance benefits. It is observed that for every 220lb of mass reduction in the vehicle structure, approximately 0.0009 to 0.0017 gal/mile of fuel can be saved depending on the type of engine [7].
- Lighter vehicles are deemed as important for the success of several DOE Energy Efficiency (DOE-EE) projects, which call for efficient and environmentally safe vehicles.
- Consumer preferences limit the vehicle downsizing options available to automakers, consequently pushing them to develop newer and efficient techniques for lightweight designs.

- Environmental, Safety, and Health (ES & H) regulations from the government necessitate development of fuel-efficient vehicles for the much needed realization of reducing global warming by minimizing the use of conventional energy resources.

Two basic approaches to vehicle weight reduction are:

1. Improving automotive design techniques
2. Development and application of new lightweight materials for vehicle design

There is an on-going trend towards using lighter metals and their alloys in manufacturing automotive components and body. The most commonly used materials are aluminum, magnesium, and their alloys, including high-strength steels. Usage of these new high tech materials results in 60% lighter weight components as opposed to the conventional low-carbon or "mild" steels [7].

Steel has been used as a dominant material for automotive manufacturing in the industry for several years. Steel provides the necessary rigidity and strength to automotive bodies. It also contributes to passenger safety during car accidents. In order to compete with the new generation of alternative light weight materials the steel industry has initiated several projects that promise to advance the steel used in automotive design. Projects such as ULSAB, ULSAC (Ultra Light Steel Auto Body, Closures respectively) and LTS (Light Truck Study) have demonstrated significant weight reduction and performance improvement potential of automotive sheet-steel [12, 13, 15].

The Partnership for a New Generation of Vehicles (PNGV) [8, 11] is a successor of ULSAB, and targets to build the next generation of light weight vehicles capable of delivering 80 miles per gallon fuel economy at 2000lb curb weight. Current research

activity in the field of lightweight structures focuses on methodologies for layout, design and analysis. Factors such as deformation, stress responses, and load carrying capacity, etc., are studied and analyzed.

1.2 Approaches to vehicle weight reduction

Several techniques have been demonstrated and utilized in the past to achieve vehicle weight reduction. A survey conducted by Kobe Steel company [14] categorizes these techniques as follows.

- Material Selection: Use of appropriate materials for vehicle design will lead to significant weight savings. Two separate methodologies for such a design are a) Reducing the thickness of existing materials, which relies on improved strength, corrosion resistance and quality of such materials, and b) Employing light weight materials such as aluminum and titanium alloys.
- Design Technology: Optimization of parts and wall thickness in accordance with application conditions proves to be an effective method for saving weight. It's essentially a redesign process which can be validated by using structure analysis and strength analysis software. This process enables quick and accurate analysis of material structure and re-evaluation of strength when the parts are redesigned.
- Manufacturing Technology: Highly functional materials needed for reducing weight demand development of advanced processing technology. There has been significant improvement in rolling, extrusion, precision casting, and forging techniques to meet increased precision of profiles.

1.3 Overview

This thesis incorporates an innovative approach that couples a newer design technique with an appropriate material selection. The technique is applied to the back panel of a Ford F-150 pickup truck. The main objective is to optimize the design of the back panel

over its current model, this consists of a sheet metal with corrugations supported by beams on the top and bottom, and the sides. The main requirements of the redesigned model are to weigh less than the original model, and to preserve its structural stability.

The redesign process used in this thesis is based on the theory of *semi-tension fields*. The theory was originally applied for the design of aircraft structures and was proved to be more effective than traditional design practices. The span of an aircraft's wings usually comprises of an upper and a lower flange connected by thin stiffened webs. Thin webs buckle under shear stresses at a fraction of their ultimate load, becausethey are relatively weak under compression and the compressive stress eventually reaches the buckling stress. Standard practice assumes that shear-webs lose their load-bearing capacity when the web buckles under load. However, a theory originally proposed by Wagner [10] demonstrated that the thin web, as opposed to the shear-resistant web, does not really fail when it buckles; it develops a series of diagonal folds, which function as a series of tension diagonals. Consequently, the thin web continues to carry the load, even after buckling. Based on this theory, buckling of the webs is permitted in aircraft structures unlike the standard structures.

Hence, the concept of semi-tension fields is essentially a post-buckling phenomenon in which the web continues to carry the load even after buckling. The advantage of semi-tension fields is two-fold: first, by using this theory the structural stability of the original structure is retained, and secondly, it replaces a comparatively heavy-weight shear-resistant web with thin webs, consequently resulting in reduced weight.

Semi-tension fields theory is applied to the back panel of the F-150 prototype truck, and the resultant model is investigated for possible weight benefits. The model of the back panel is drawn and analyzed using IDEAS Master Series 8 FEA Package. As previously discussed, semi-tension field theory is a concept that was originally applied to the design of aircraft structures. The same theory is now applied to the design of automotive structures on an experimental basis in order to evaluate the resultant weight savings. A static analysis of the back panel gives an estimate of the maximum load that it can carry under the given boundary conditions. Few other problems related to the redesign are also studied, analyzed and presented in the thesis. Finally, weight savings due to this new design are discussed.

1.4 Motivation

The IMPACT (Improved Materials for Power train Architectures for 21st Century Trucks) program is a collaborative effort among various industrial, government, and academic organizations. The program aims to develop robust light-weight and dual-use trucks, using higher-strength, low cost steels and optimized designs [6]. The first phase of this three-phase program established that cost-effective weight reductions of up to 25% are possible using steel, since it offers the most structural benefit per unit cost [5]. The second phase of the program consists of designing and prototyping vehicles, which achieve up to 25% weight reduction without compromising the other vehicle parameters. The initial design and analysis of these prototypes is based on the Ford F-150 pickup trucks. This thesis partially contributes towards the second phase of this program, and focuses on an opti-

mized design for the back panel of the prototype F-150. The motivation for this thesis comes from the fact that semi-tension fields theory has not been considered in the past for its applicability to automotive structures. This thesis is an attempt to apply the theory to the back panel of F-150 pickup truck in anticipation of further weight savings over the current model. Hence the driving motivation for this thesis comes from the coupled effect of the following factors: 1. Current efforts by the auto industry to achieve weight reduction by optimizing certain parts of the vehicle, without compromising stability, need to be complemented with further academic research. 2. Semi-tension fields theory, which was successfully applied in the past to aircraft designs, and proved to achieve weight savings, remains as an unexplored area for automotive construction.

1.5 Hypothesis and Basis

This thesis proposes to optimize and enhance the current design of the back panel of the F-150 pick up truck in order to achieve significant weight savings, consequently improving its performance and fuel economy. The hypothesis of this work is that applying the theory of semi-tension fields to the redesign of the back panel of the truck enables weight reduction, without affecting its structural stability. The previous success of semi-tension field theory in the aircraft industry is the basis for this thesis. The results of this thesis give a general impression regarding the applicability of semi-tension field theory in the automotive industry. The validity and the subsequent applicability of the theory will rely on a successful analysis of the back panel of the F-150 prototype truck under the current

study, plus possibly extending it to other parts of the vehicle, and other models as well in the future.

CHAPTER II

THEORY OF SEMI-TENSION FIELDS

2.1 Introduction

The design and development of structures is rapidly progressing with increased availability of new materials. Various types of structures and design techniques are continually researched and studied in order to devise efficient designs that minimize weight without affecting the stability of the structure. The current study focuses on one such design methodology, which was originally applied in the design of aircraft structures. The current design is based on the principles of semi-tension fields theory.

The theory of semi-tension fields was originally developed by Wagner [3] based on an observation of a phenomenon that occurred in thin webs under shear load. Thin webs are generally used in the design of aircraft wings, which typically consist of an upper flange and a lower flange fastened by thin webs. Standard structural design theories previously assumed that thin webs tend to buckle under shear stresses even before the ultimate load is reached. Buckling of the web is caused due to diagonal compressive stresses. This results in a wrinkling type of a structure as shown in figure 2.1 [10], which can support only the diagonal tensile stresses, in a direction perpendicular to the buckling direction.

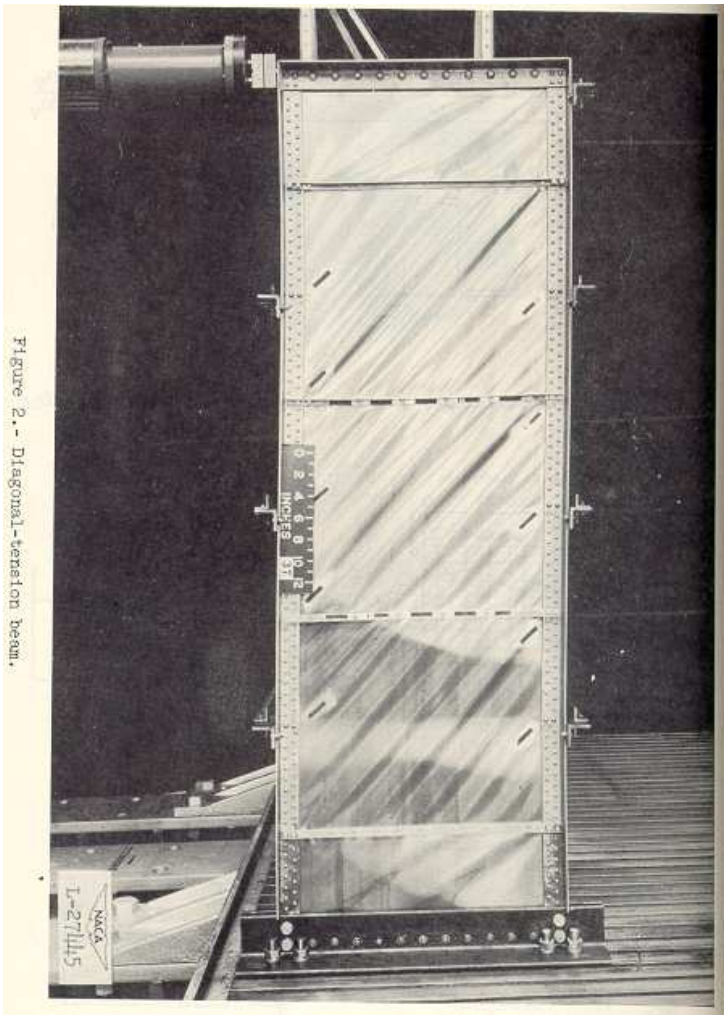

Figure 2.1 Severe wrinkling of the web.

From reference [10]

This type of beam is referred to as a *complete tension field beam or pure tension field beam*. A diagonal tension beam is defined as a thin web that buckles into diagonal wrinkles much below the design (failing) load.

2.2 Complete tension field beams

Standard structural design principles assume that when the web buckles, the shear web loses the ability to hold the load bearing capacity and eventually it fails. Wagner proved with reasoning and experiments that a thin web with transverse stiffeners does not really fail when it buckles. The thin buckled web develops wrinkles, which act as diagonal tension field. The compressive forces in the stiffeners resist the tendency of tensile stresses to pull the beam flanges together [1, 10].

The action of a tension field beam is explained using a simple structure such as a single bay truss with double diagonal members (A) and (B) carrying an external load P. For small values of P, both the diagonal members carry equal and opposite stresses; tensile and compressive respectively. As the load P is increased, at a certain limit the compressed diagonal member A cannot take further load, and consequently it buckles. However, the other member, being in tension, can take further load until it reaches its ultimate strength. Therefore, any increase of the shear due to increase of external load P, after one of the members has buckled, is handled by the additional diagonal bracing provided by the tensile member.

Based on the above theory, a similar structure, obtained by replacing the two diagonals by a flat sheet web (figure 2.2), is studied for tension field action.

Under a small load P, web does not buckle and both the tensile and compressive stresses equal the shear stress in the web at this point. Practically, the sheet is in a state of pure shear with tensile and compressive stresses at 45^0 to the axes. The thin flat sheet, be-

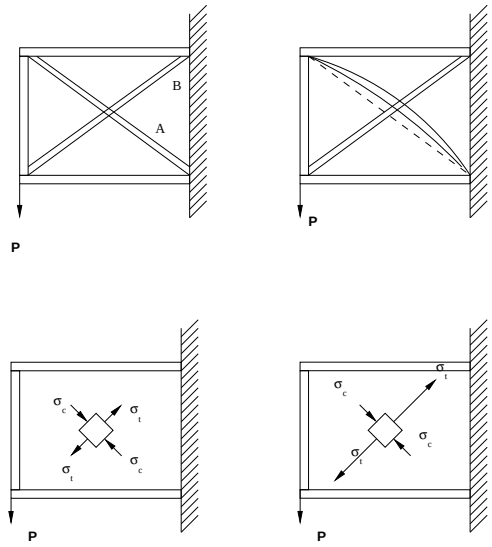

Figure 2.2 Diagonal Tension Field Action.

ing relatively weak in compression, buckles when the compressive stress reaches buckling stress as load is increased. However, the panel does not collapse because further increase in load is handled by increase in diagonal tension of the sheet web. As the load P reaches a critical value, the tensile stresses become prevalent over compressive stresses.

Since the shear load on the panel is transferred by diagonal tension in the web and due to efficiency of flat sheet in tension, this method of carrying shear load allows the use of relatively thin webs.

2.3 Pure tension field beams

Two types of webs have been primarily considered as guiding reference over the years for use in design practices [10]. The first type, *Shear resistant* webs, are those in which

Table 2.1 Parameters relevant to figure 2.2

P	Shear load on the panel
A	Diagonal member in compression
B	Diagonal member in tension
σ_c, σ_t	Compressive and tensile stresses in members

buckling does not take place before failure. The second type is called *Pure diagonal tension* web, which is a theoretical limiting case, in which buckling of the web takes place at an infinitesimally small load. The weight saving opportunity in automobiles comes about because virtually all automotive structures have shear resistant beam webs which are heavier than semi-tension field webs, pure diagonal tension can be only approached asymptotically. It has been found that the state of pure diagonal tension is approached when the applied load is several hundred times the buckling load [10]. In a typical scenario, the ratio of failing load to the buckling load is very low. For lower values of this ratio, the theory of pure diagonal tension gives poorer approximations. Hence, for this thesis, the web is considered to fall into an intermediate category of *incomplete diagonal tension or semi-tension fields*. It was observed that semi-tension field webs could withstand some diagonal compressive stress after buckling, so that before the time of failing they act in an intermediate range between shear resistant webs and pure tension field webs [2].

2.4 Basic Mathematical formulation for pure-tension fields

An elementary approximation of the beam equations, which were developed by Wagner is presented in this section from reference [1]. A cantilever beam with parallel chords and vertical stiffeners subjected to single shear load V at its free end is considered for the following derivations.The dashed lines in the figure 2.3 indicate the wrinkling when the web buckles.The vertical and horizontal shearing stress is constant and is given by

$$\sigma_s = V/ht \tag{2.1}$$

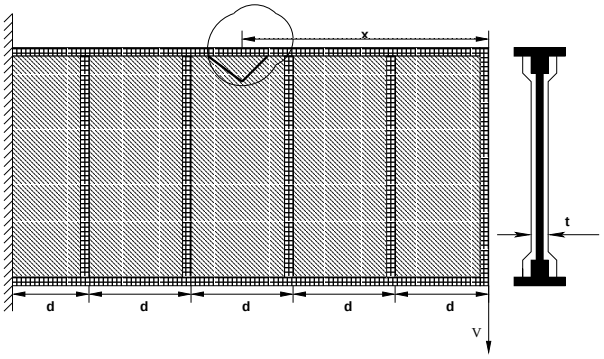

Figure 2.3 Cantilever loaded at its end.

Free body diagram (figure 2.4) of a small segment of the web is drawn and analyzed for equilibrium.

Table 2.2 Determination of shearing stress for the cantilever beam

t	Web thickness
h	Distance between the centroids of flange rivets
V	Vertical shear load
σ_s	Shear stress

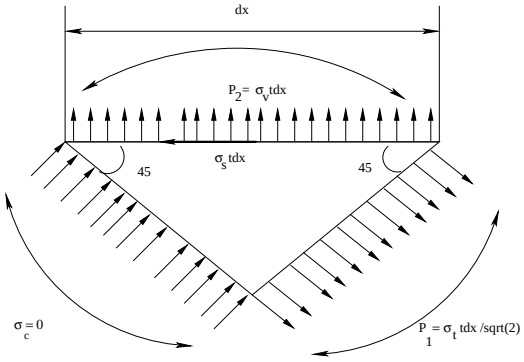

Figure 2.4 Free body diagram of a segment on the uppermost layer of beam.

The thin web, being weak in compression, can carry very small loads in compression before buckling. Therefore, compressive stress on the small segment is neglected. Hence,

$$\Sigma F_X = 0 \Rightarrow -\sigma_s t dx + (\sigma_t dx/\sqrt{2}) * 1/\sqrt{2} = 0 \tag{2.2}$$

From the shearing stress equation 2.2, $\sigma_t = 2\sigma_s = 2V/ht$ Similarly,

$$\Sigma F_Y = 0 \Rightarrow \sigma_v t dx - (\sigma_t t dx/\sqrt{2}) * 1/\sqrt{2} = 0 \tag{2.3}$$

Hence $\sigma_t = 2\sigma_v$. Therefore $\sigma_v = \sigma_s$.

Table 2.3 Determination of forces acting on the sheet element

t	Web thickness
h	Distance between the centroids of flange rivets
V	Vertical shear load
σ_s	Web shearing stress
σ_t	Web tensile stress

Rivets attach stiffeners and flanges to the web and they are subjected to an axial load and a normal load each being equal to $\sigma_s t dx$. Therefore, The resultant force = $\sqrt{2}\sigma_s t dx$ For one inch of the segment, resultant load will be $\sqrt{2}\sigma_s t$.

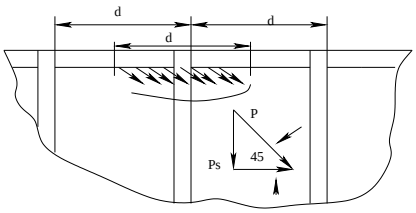

Figure 2.5 Stiffener Load Calculation.

The web in the tension field beam action tends to pull the flanges together and this is prevented by vertical stiffeners attached to the web. Thus, uprights serve as compression posts. Uprights are acted upon by an axial compressive load P_s which is equal to the vertical web tensile stress over a distance d.

Table 2.4 Stiffener load calculation

t	Web thickness
h	Distance between the centroids of flange rivets
V	Vertical shear load
σ_s	Web shearing stress
σ_t	Web tensile stress
P_s	Axial compressive load
P	Tensile Load
d	Distance between stiffeners

From figure 2.5 $P_s = P \sin 45^0$ Where: $P = \sigma_t dt/\sqrt{2}$ Hence, $P_s = \sigma_t dt/2 = Vd/h$ A free body diagram (figure 2.6) of a portion of the beam at a distance x from an end is drawn and analyzed.

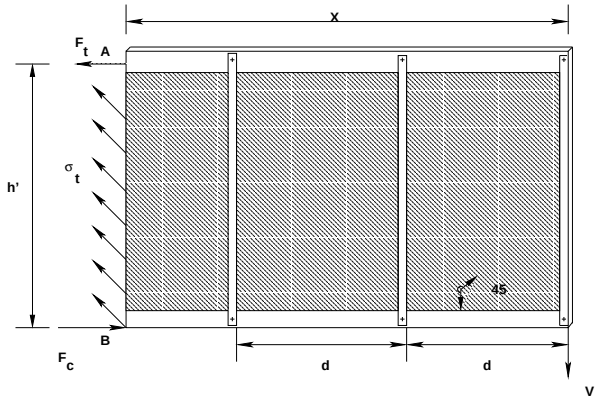

Figure 2.6 Determination of flange axial loads.

Equating internal and external bending moments,

$$\Sigma M_B = M_X - F_t h' - \sigma_t \cos 45^0 h' t \cos 45^0 h'/2 = 0 \qquad (2.4)$$

Table 2.5 Flange axial load calculation

t	Web thickness
h'	Distance between the centroids of flanges
V	Vertical shear load
σ_s	Web shearing stress
σ_t	Web tensile stress
M_x	External bending moment at Section AB
F_t	Tensile flange axial load
F_c	Compressive flange axial load
d	Distance between stiffeners

$$\sigma_t = 2\sigma_s \Rightarrow \sigma_s = V/h't \Rightarrow \sigma_t = 2V/h't \tag{2.5}$$

Substituting,

$$M_X - F_t h' - Vh'/2 = 0 \Rightarrow F_t = M_X/h' - V/2 \tag{2.6}$$

$$\Sigma X = 0 \Rightarrow F_c = M_X/h' + V/2$$

Due to bending, compressive flange axial load increased by V/2 and tensile load decreased by V/2(due to horizontal component of web tension field).

2.5 General equations for tension field beams

The earlier section was an elementary derivation of various stresses under complete tension field action where the angle of diagonal tension α was assumed to be 45^0. Practically, the angle of diagonal tension is not 45^0, but depends on other factors such as flange areas, beam height, stiffener spacing, etc. [1]

The equations to determine stresses for a general case are given as below

Diagonal tensile stress in web:

$$\sigma_t = (2V/ht) * 1/\sin 2\alpha \tag{2.7}$$

Flange axial load in tension:

$$F_t = M/h' - (V/2) * \cot\alpha \tag{2.8}$$

Flange axial load in the compression:

$$F_c = M/h' + (V/2) * \cot\alpha \tag{2.9}$$

Axial force in the stiffeners:

$$F_{stiff} = -(Vd/h)\cot\alpha \tag{2.10}$$

Figure 5.— Secondary actions in diagonal—tension beams.

Figure 2.7 Web Stress Concentration.

From reference [10]

The above equations are based on the assumption that the flanges were infinitely stiff in bending. But the flanges due to the lateral pull of web tension field, will act as a

Table 2.6 Parameters for tension field equations

t	Web thickness
h'	Distance between the centroids of flanges
h	Distance between the centroids of flange-web rivets
V	Vertical shear load
α	angle of diagonal tension
σ_s	Web shearing stress
σ_t	Web tensile stress
M	External bending moment
F_t	Tensile flange axial load
F_c	Compressive flange axial load
F_{stiff}	Axial force in stiffeners
d	Distance between stiffeners
R	Correction factor due to web stress concentration
A_u, A_L	Areas of upper and lower flanges
A_s	Area of stiffener
I_u, I_L	Moment Of Inertia of upper and lower flanges

continuous beam over the stiffeners as supports as shown in figure 2.7. The deflections of the flanges relieves the web stress in the center and concentrates near the stiffeners where the deflection of flanges is prevented.

A correction factor R to take care of the web stress concentration due to flange deflection was developed by Wagner[3]. This factor R can be determined by calculating the flange-flexibility w_d and looking up a corresponding value of R in the graph as shown in figure 2.8.

$$w_d = 1.25d \sin\alpha \sqrt[4]{t/(I_u + I_L)h} \tag{2.11}$$

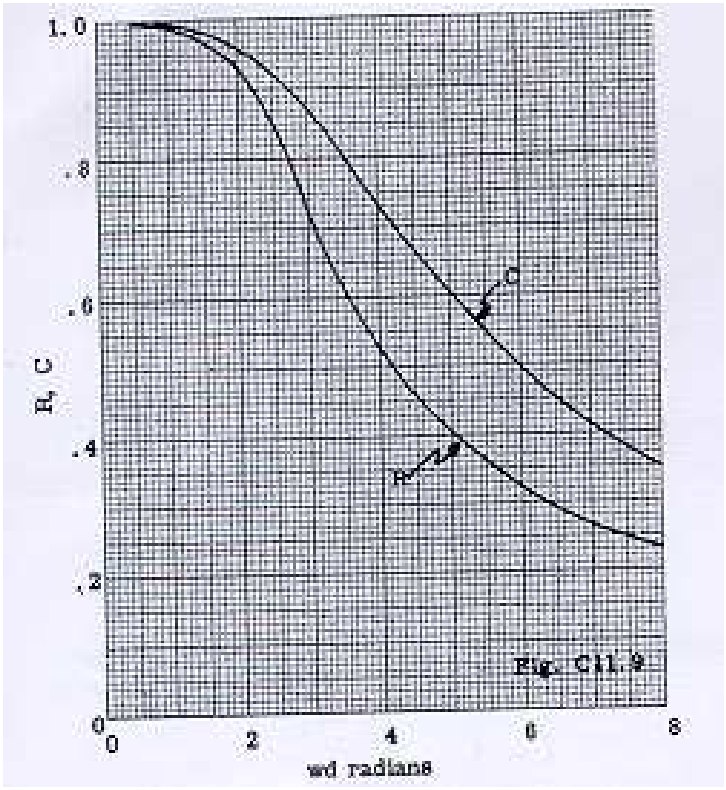

Figure 2.8 Relation between Correction Factor R and w_d.

From reference [1]

Web angle is determined as follows:

$$a = \frac{1 + \frac{ht}{A_u + A_L}}{\frac{dt}{A_s} - \frac{ht}{A_u + A_L}}$$

$$\sin^2 \alpha = \sqrt{a^2 + a} - a \tag{2.12}$$

2.6 Modified Wagner equations

In the development of the basic equations outlined previously, Wagner made several conservative assumptions such as that the shear strength of beam flanges and the shear carried by the web before it buckles are negligible. The modified Wagner equations consider that the remaining beam shear is actually carried by the web in the form of diagonal tension field, which is obtained by subtracting the above two factors.

2.6.1 Shear load carried by flanges

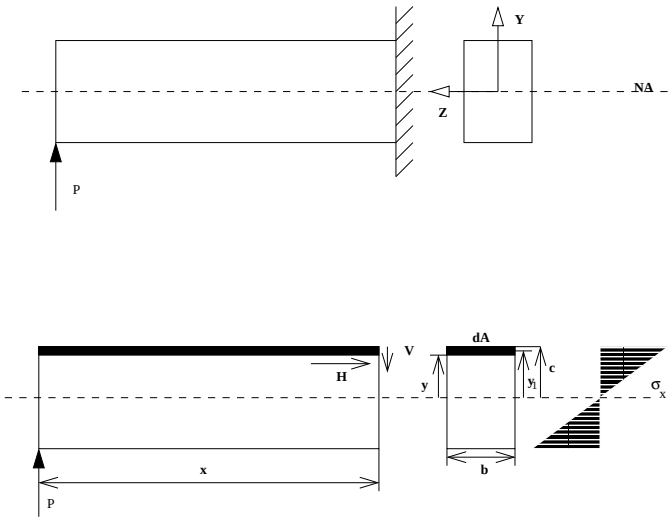

Figure 2.9 Flexural shear stress and shear flow.

A cantilever beam with rectangular cross-section is chosen to demonstrate the procedure involved in determining the shear load. As shown in figure (2.9), load P is applied

at one of its ends. The force acting on the element due to the stress σ_x is given by the equation:

$$F = \sigma_x dA = \frac{M y dA}{I} \tag{2.13}$$

Therefore, force acting on the left edge of the element can be calculated as

$$F_{1x} = \int_y^c \frac{My}{I}\, dA \tag{2.14}$$

Force acting on the right edge of the element is equal to

$$F_{2x} = \int_y^c \frac{M + dM}{I}\, y dA \tag{2.15}$$

Hence, difference in forces can be determined as

$$F_{2x} - F_{1x} = \tau b dx = \int_y^c \frac{M + dM}{I}\, y dA \; - \int_y^c \frac{My}{I}\, dA \tag{2.16}$$

where τ is the shear stress.

$$\tau b dx = \int_y^c \frac{dMy}{I} dA \tag{2.17}$$

$$\tau = \frac{dM}{dx}\frac{1}{Ib}\int_y^c y dA \tag{2.18}$$

The loading function q(x) can be expressed as

$$q(x) = \frac{dV}{dx} = \frac{d^2M}{dx^2} \tag{2.19}$$

The term dM/dx = V based on the above equation. Therefore, $\tau = \frac{VQ}{Ib}$ where Q equals the static moment of area denoted by $\int_y^c y dA$ It is assumed the shear stresses are approximately constant between the centroids of the flange-web rivets. Therefore, Q in the above equation equals the static moment of flange area and I equals moment of Inertia of flange area about

neutral axis. Static moment of area of flanges dominates over the static moment of area of flanges + web. Hence static moment of area of flanges is chosen for determining the total shear load and same is the case for moment of Inertia.

The shear load resisted by web alone is given by

$$V_w = VQh/I \tag{2.20}$$

where, h is the effective web depth or the distance between the centroids of flange web rivets.

Therefore, the total shear load resisted by both flange and web is equal to

$$V = V_w I/Qh \tag{2.21}$$

Hence the difference between the total shear load and that carried by the web gives the shear load carried by the flanges.

2.6.2 Shear load carried by web

Until the point when the web buckles, shear stress distribution is assumed to be constant over the web. But when the web buckles, the web can practically hold the compressive stress but cannot increase it. With increase in the shear load resistance is provided by the increase in diagonal tension field. Therefore, for loads after the web has buckled, web is in a state of pure tension field beam, because the compressive shear stress is relatively insignificant compared to the tensile stress.

2.6.2.1 Shear load carried by web at web buckling point

From the figure 2.10, the vertical shear stresses have been replaced by diagonal tensile and compressive stresses each equal to the critical shearing stress. Hence the shear load (V_{cr}) carried by web at the web buckling stress equals

$$V_{cr} = \sigma_{s_{cr}} ht$$

The critical shear buckling stress ($\sigma_{s_{cr}}$) is given by:

$$\sigma_{s_cr} = \frac{\pi^2 k_s E(t/b)^2}{12(1-\nu^2)}$$

Where, k_s is a function of the aspect ratio a/b of the panel and the edge conditions.

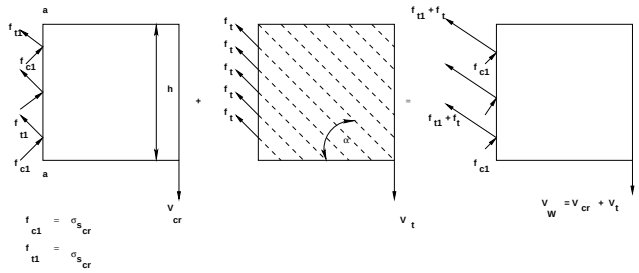

Figure 2.10 Critical stress at web buckling point.

2.6.2.2 Shear load carried by web after buckling

When the shear load increases beyond the web buckling stress, web buckles down into a tension field and the diagonal tensile stress tends to pull the flanges together and thus cause bending in the flanges. The diagonal tensile stress σ_t for shear resistant web does

Table 2.7 Calculation of the total shear load developed by web after buckling

σ_{t_max}	Maximum combined tensile stress in the web
σ_t	Diagonal tensile stress
σs_{cr}	Critical shear buckling stress
σ_{ty}	Yield strength of the material
R	Concentration factor
I	Moment of Inertia of section
Q	Static moment of area of flanges

not produce such action, therefore, a concentration factor 1/R must be multiplied to the tensile stress σ_t. Hence,

$$\sigma_{t_max} = (\sigma_t/R + \sigma_{s_{cr}}) \Rightarrow \sigma_t = (\sigma_{t_max} - \sigma_{s_{cr}})R$$

The vertical component of the diagonal tensile stress equals the shear load developed by the web after buckling. shear load V_t is obtained as(from equation 2.7)

$$V_t = (\sigma_{t_max} - \sigma_{s_{cr}})Rht \sin\alpha \cos\alpha \tag{2.22}$$

Total shear load developed by the web after buckling V_{ty} when the maximum stress equals the yield stress(σ_{ty}) can be calculated as:

$$V_{ty} = (\sigma_{ty} - \sigma_{s_{cr}})Rht \sin\alpha \cos\alpha \tag{2.23}$$

Total yield shear resistance (V_{W_ty}) of the web equals:

$$V_{W_ty} = (V_{cr} + V_{ty}) \tag{2.24}$$

Therefore total beam shear resistance can be calculated as:

$$V_{yield} = \frac{I(V_{cr} + V_{ty})}{Qh} \tag{2.25}$$

2.7 Flange loads calculation

Axial flange loads are primarily caused by the stresses due to primary bending of the beam according to the flexural theory and also due to stresses produced by the tension field. Bending of the flanges because of the tension field also produces additional stresses that are termed as secondary bending stresses.

Stresses due to primary bending: Bending stress can be determined using the following equation:

$$\sigma_b = \pm\frac{M_{cr}y}{I} \pm \frac{(M - M_{cr})y}{I_F} \tag{2.26}$$

The first term in equation 2.26 represents the bending stress till the point where the web breaks down into a tension field and thus the web is still effective in computation of moment of inertia. The second term denotes the bending stress when the beam acts as a tension field web. Therefore, the buckled web is assumed to be ineffective in calculating moment of inertia.

Table 2.8 Calculation of stresses due to primary bending

I	Moment of Inertia of total section about neutral axis
I_F	Moment of Inertia of section without web about neutral axis
M_{cr}	Bending moment for load which causes web buckling
M	Total bending moment on section
σ_b	Bending stress

Flange axial stresses due to tension field: The upper and lower flanges are subjected to a compressive load, due to the horizontal component of the tension field, which is equal to

$$F_H = -\frac{V_t}{2}\cot\alpha$$

Table 2.9 Calculation of flange axial stresses

V_t	Shear load carried by tension field action
α	Angle of diagonal tension
F_H	Compressive and tensile flange loads respectively

Secondary Bending Stresses: In order the compute the secondary bending moments due to lateral pull of tension field, the flange is treated as a continuous beam with spans equal to stiffener spacing. The component of the web diagonal tensile stresses normal to flange is equal to

$$w_v = \frac{V_t}{h}\tan\alpha$$

The moment(average) over the supports, for a continuous beam of equal spans, is calculated as:

$$M_{avg} = \frac{1}{12}w_v d^2$$

The deflections of the beam flanges relieves the web stress in the midportions of the panels which reduces the continuity moment over the support. A relieving factor C is introduced

to be used when calculating the moment. Therefore, secondary bending moment(average) on flanges is

$$M_{sec} = \frac{1}{12} C \frac{V_t}{h} d^2 \tan \alpha \tag{2.27}$$

Table 2.10 Calculation of secondary bending moment on flanges

V_t	Shear load carried by web in diagonal tension
α	Angle of diagonal tension
M_{sec}	Secondary bending moment on flanges
C	Relieving factor
d	Spacing between stiffeners

CHAPTER III

FINITE ELEMENT ANALYSIS

3.1 Analysis of Current Back Panel

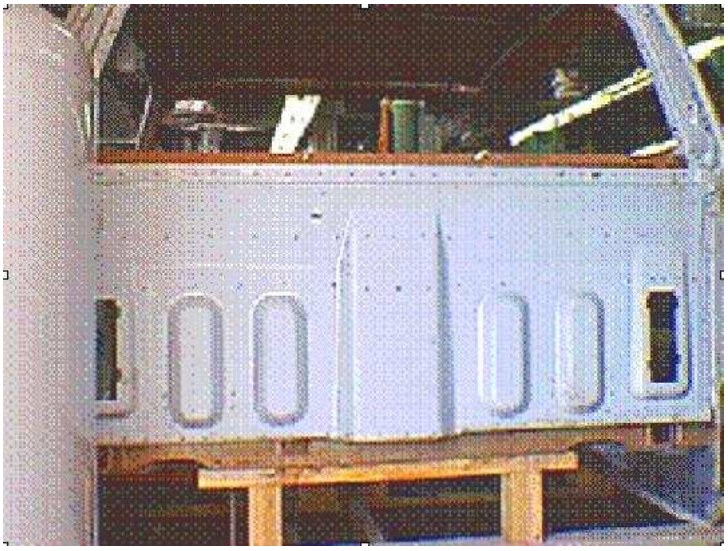

Figure 3.1 Snap shot of the Back Panel.

The current design(3.1) of the back panel of prototype F-150 pick up truck consists of a corrugated sheet supported by beams on either sides, top and bottom. The idea is to implement the concept of semi-tension fields to design a completely new back panel with reduced weight while retaining the benefits of the current model. Initial step towards

designing the new model would be to determine the design load that the panel has to be designed to. A Finite Element Analysis has been performed on the current panel subjected to a unit shear load. Thus, the design load can be calculated based on the maximum stress of the back panel.

The new design of back panel is based on semi-tension field theory. In order to permit semi-tension field action the existing panel has to be replaced by a thin continuous sheet web supported by vertical stiffeners.

Calculation of Design Load:

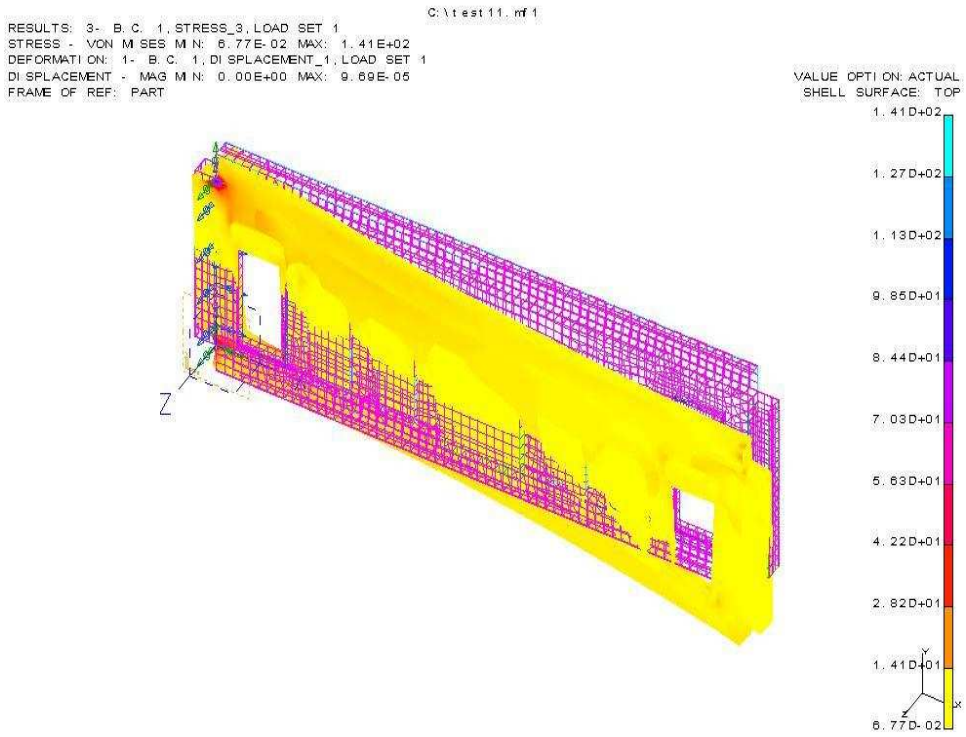

Figure 3.2 Calculation of Design Load.

From figure 3.2, it is observed that the highest value of stress is equal to 141psi. But, this value corresponds to those locations which are subjected to either the loading or boundary conditions. Hence, the value that is prevalent over the entire panel uniformly is chosen for the purpose of the calculation of design load. Maximum stress from Finite Element Analysis of Panel, for a unit load = 28.1 psi

Maximum allowable stress is calculated assuming a factor of safety 2 = Yield Strength/Factor of Safety = 24000/2 = 12000 psi

Hence design load for this material = Max. allowable stress/ Max. stress = 12000/28.1 = 427 lb

Calculation of thickness:

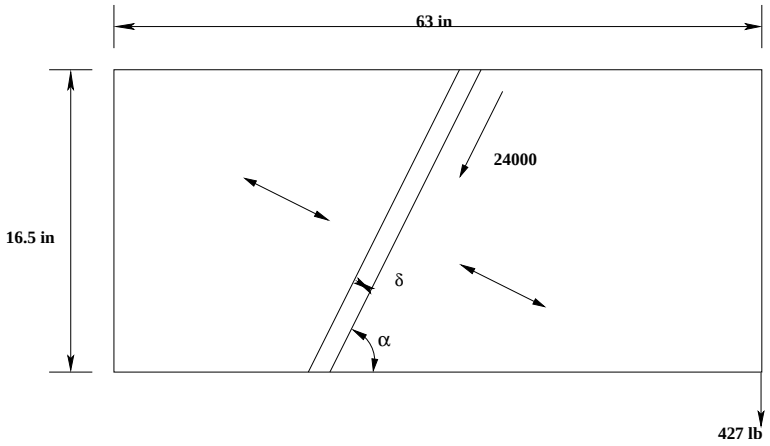

Figure 3.3 Calculation of thickness.

As shown in figure 3.3, only the web, without the flanges and vertical stiffeners, is chosen in order to determine the optimum value of thickness that can withstand the loading

conditions. It should also be noted that for this calculation, the height of the panel does not include the flanges. An infinitesimal element(see figure 3.3)of width δ and thickness t is chosen for the following calculations.

Total shear load on the back panel = 427 lb

Width of the element = 63*sinα in

Applying conditions of equilibrium to the element,

$$24000 * 63 * \sin\alpha * t * \sin\alpha = 427 \tag{3.1}$$

Referring to equation 2.12,

$$\sin^2\alpha = \sqrt{a^2 + a} - a$$

From equation 2.5,

$$a = \frac{1 + \frac{ht}{A_u + A_L}}{\frac{dt}{A_s} - \frac{ht}{A_u + A_L}} = \frac{1 + 24.47 * t}{41.77 * t}$$

Substituting the values of "a" and "$\sin^2\alpha$" in the equation 3.1, equation simplifies to

$$24.47 * t^2 + 0.986 * t - 0.00056834 = 0$$

Only positive root value t = 0.000568.

Thickness t = 0.0006in This is a case of over design since thickness values lower than 0.02 in are not allowable. Therefore, thickness is chosen to be = 0.02 in.

Table 3.1 Calculation of thickness according to the new design

d	Stiffener spacing	15.5in
A_u, A_L	Area of upper and lower flange	0.3985 in^2
A_s	Area of the stiffener	0.23 in^2
A	Area of cross-section of upper and lower flanges	0.44 in^2

3.2 Strength Analysis of Web and Flanges of the New Back Panel

Figure 3.4 shows the proposed new design of Back panel, which consists of a thin web of thickness 0.02 in supported by three vertical stiffeners and the upper and lower flanges(shown in fig 3.5).

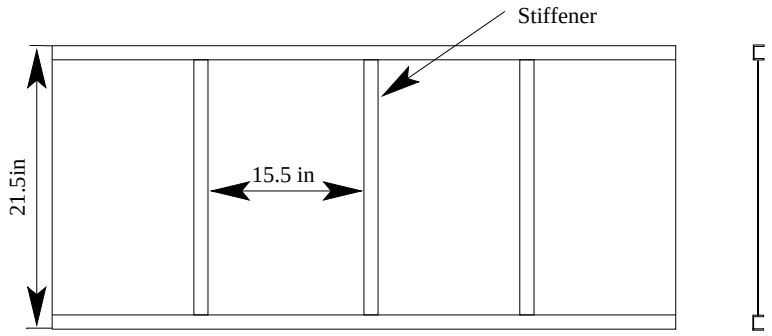

Figure 3.4 Proposed new design of the Back Panel.

From the mathematical review in chapter II, various parameters can be determined as follows:

Critical buckling stress is given by

$$\sigma_{s_{cr}} = \frac{\pi^2 k_s E(t/b)^2}{12(1-\nu_e^2)} = 261.83psi.$$

critical shear load $V_{cr} = \sigma_{s_{cr}} * h * t$ = 99.495 lb

Table 3.2 Parameters for calculation of critical buckling stress

k_s	Shear buckling coefficient	5.8
E	Elastic modulus of the material	$3.00 * 10^7$
t	Thickness	0.02in
b	Distance between the stiffeners	15.5 in
ν	Poisons ratio	0.3

Determining angle of diagonal tension:

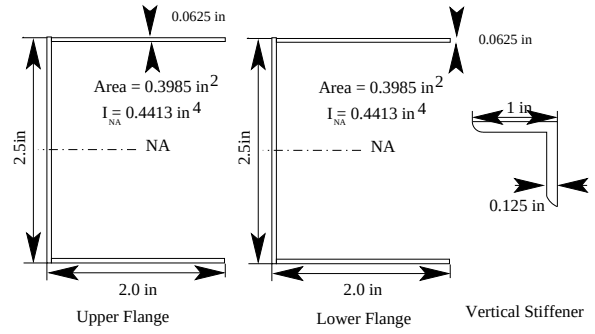

Figure 3.5 Upper,Lower Flanges and Vertical Stiffener.

This requires calculation of value 'a', which can be calculated as follows:

Referring to equation 2.5,

$$a = \frac{1 + \frac{ht}{A_u + A_L}}{\frac{dt}{A_s} - \frac{ht}{A_u + A_L}} = 1.696$$

From equation 2.12, $\sin^2 \alpha = \sqrt{a^2 + a} - a$ thus $\sin^2 \alpha = 0.4427 \Rightarrow \alpha = 41.7^0$

Web stress concentration factor:

Table 3.3 Calculation of web stress concentration factor

d	Stiffener spacing	15.5 in
h	Distance between flange centroids	19in
t	web thickness	0.02in
R	Web stress Concentration factor	0.76
α	Angle of diagonal tension	41.7^0
I_u, I_L	Moments of Inertia of upper and lower flanges	$0.4413 in^4$

From equation 2.11,flange flexibility factor can be determined as:

$$w_d = 1.25 d \sin \alpha \sqrt[4]{t/(I_u + I_L)h} = 2.394$$

The web stress concentration factor can be determined as R = 0.86 from the graph in figure 2.8

Shear Load carried by web after buckling:

Table 3.4 Calculation of total shear load

d	Stiffener spacing	15.5 in
h	Distance between flange centroids	19in
R	Web stress Concentration factor	0.86
α	Angle of diagonal tension	41.7^0
I_{NA}	Moment of Inertia of the section about NA	$72.81in^4$
Q	Static moment of area of flanges	$3.786in^3$
V_{cr}	Shear load resistance developed by web up to buckling	99.495lb
$\sigma_{s_{cr}}$	Critical buckling shear stress	261.83

For Mild steel, Yield stress in tension is equal to 24000 psi(σ_{ty}) Shear strength of the web acting as tension field after buckling is given by:

$$V_{ty} = (\sigma_{ty} - \sigma_{s_{cr}})Rht \sin\alpha \cos\alpha$$

$$\Rightarrow V_{ty} = (24000 - 261.83) * 0.76 * 19 * 0.02 * 0.6652 * 0.7466 = 3852.74lb$$

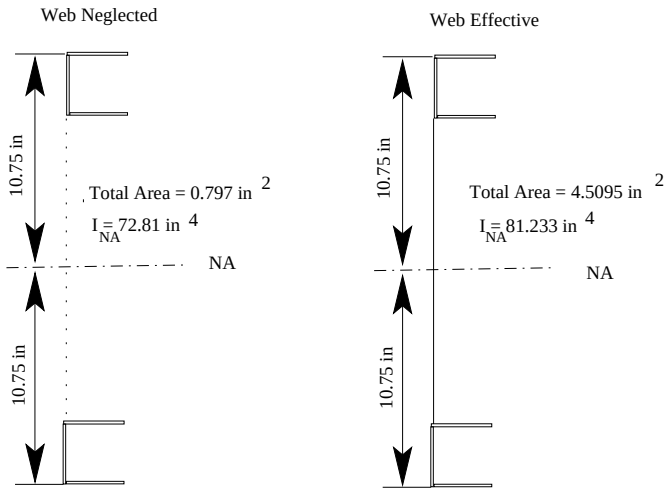

Figure 3.6 Calculation of Moment of Inertia.

Moment of Inertia I is computed as I_{NA}(Moment of Inertia of section without web) = $I_{u_C} + A_u * d^2 + I_{l_C} + A_l * d^2$= (0.4413 + 0.3985*9.5*9.5)*2 = 72.81 in^4

Static moment of flange area about the Neutral Axis $Q = \int ydA = 0.3985 * 9.5 = 3.786 in^3$

Total shear load including strength of flanges is given by equation 2.21,

$$V_{yield} = \frac{I(V_{cr} + V_{ty})}{Qh}$$

$V_{yield} = (72.81)(3404.75 + 99.495)/(3.786 * 19) = 4000.365 lb$

The results show that the beam shear resistance can be proportioned as:

Carried by the web in pure shear = $V_{cr}/V_{yield} = 99.495 * 100/4000.365 = 2.5\%$

Carried by the web as a diagonal tension field = $V_{ty}/V_{yield} = 3852.74 * 100/4000.365 = 96.3\%$

Remaining 1.2 $\%$ is carried by the shear strength of the flanges

Due to the thin web thickness, web buckles at a relatively low stress, thus the percent of the external shear carried by web at buckling is quite small.

Flange Strength Analysis: Design bending moment is calculated to be M = 427*63 = 26901 lb-in.

The bending moment due to a shear of 99.495 lb will be resisted by the entire cross-section and the web = $M_{cr} = 99.495 * 63 = 6268.19 lb - in$

Table 3.5 Calculation of bending stresses

M	Design bending moment	26901 lb-in
M_{cr}	Bending moment due to the shear load	6268.19 lb-in
y	Distance from neutral axis	10.75in
I	Moment of Inertia of total section about NA	81.233in^4
I_F	Moment of Inertia of section without web	72.81in^2
$\sigma_{b_{UF}}$	Upper flange bending stress	3875.825psi
$\sigma_{b_{LF}}$	Lower flange bending stress	-3875.825psi

Bending moment for tension field beam $(M - M_{cr})$ = 26901 - 6433.2 = 20632.81 lb-in

Upper Flange Bending Stresses: Referring to equation 2.26,

$$\sigma_{b_{UF}} = \frac{-(-6268.19 * 10.75)}{81.233} + \frac{-(-20632.81.8 * 10.75)}{72.81} = 3875.825psi$$

Lower Flange Bending Stresses:

$$\sigma_{b_{LF}} = \frac{-(-6268.19 * -10.75)}{81.233} + \frac{-(-20632.81 * -10.75)}{72.81} = -3875.825psi$$

Average Axial Flange Loads Due to Bending:

Total Flange Load = M/h = 26901/19 = 1415.84lb

Upper Flange

$$\sigma_{t_{avg}} = 1415.84/.3985 = 3552.92psi$$

Lower Flange

$$\sigma_{c_{avg}} = -1415.84/.3985 = -3552.92psi$$

Table 3.6 Calculation of flange axial loads due to bending

$\sigma_{t_{avg}}$	Upper flange average axial load due to bending	3552.92lb
$\sigma_{c_{avg}}$	Lower flange average axial load due to bending	-3552.92lb
V_t	Shear load carried by tensile field	322.37lb
F_H	Axial load in flanges due to diagonal tension	-180.91lb
σ_t, σ_c	Average stresses on upper and lower flanges	-453.98 psi

Flange Axial Loads due to Tension Field Action:

If V_t is the shear load carried by the tensile field under the given shear load of 427 lb, then from equation 2.25,

$$427 = \frac{72.81}{3.786 * 19}(99.495 + V_t) \Rightarrow V_t = 322.37lb$$

Axial Load in each flange due to diagonal tension in the web:

$$F_H = -.5 * V_t * \cot\alpha = .5 * 322.37 * \cot(41.7) = -180.91lb$$

Average Stress on Upper Flange equals, $\sigma_t = -180.91/0.3985 = -453.98psi$

Average Stress on the Lower Flange equals, $\sigma_c = -180.91/0.3985 = -453.98psi$

Combined Flange Axial Stresses: Upper Flange Extreme Fiber:

$$\sigma_{t_e} = 3875.825 - 453.98 = 3421.845psi$$

Average Stress: $\sigma_{t_{av}} = 3552.92 - 453.98 = 3098.94psi$

Lower Flange Extreme Fiber:

Table 3.7 Calculation of flange axial loads due to tension field

σ_{t_e}	combined stress on upper flange extreme fiber	3421.845 psi
$\sigma_{t_{av}}$	average stress on upper flange	3098.94psi
σ_{c_e}	combined stress on lower flange extreme fiber	-4329.28psi
$\sigma_{c_{av}}$	average stress on lower flange	-4006.9 psi

$\sigma_{c_e} = -3875.825 - 453.98 = -4329.805psi$

Average Stress: $\sigma_{c_{av}} = -3552.92 - 453.98 = -4006.9psi$

Flange Secondary Bending Stresses: Upper and Lower flanges act as continuous beams with stiffeners as the support points under the transverse load(equal to the vertical component of the web diagonal tensile stresses.) Secondary bending moment(Average) can be approximated as $M_{sec} = 1/12 * C * V_t/h * d^2 * \tan\alpha = 279.95lbin$ where, C = .925 for w_d = 2.394

Secondary Bending Stresses on Upper Flange:

$SectionModulus(Z)$ = I/c(Lower fiber) = 0.4413/1.25 $= 0.35304$

$SectionModulus(Z)$ = I/c(Upper fiber) = 0.4413/1.25 $= 0.35304$

Table 3.8 Calculation of secondary bending stresses of upper flange

$\sigma_{b_{UFLF}}$	Upper flange bending stress on lower fiber	-792.97psi
$\sigma_{b_{UFUF}}$	Upper flange bending stress on upper fiber	792.97psi
σ_{UFLF}	Combined stress on upper flange lower fiber	2305.97psi
σ_{UFUF}	Combined stress on upper flange upper fiber	4214.815psi

Upper Flange bending stress on lower fiber $\sigma_{b_{UFLF}}$ = 279.95/0.35304 = -792.97 psi

Bending Stress on upper fiber $\sigma_{b_{UFUF}}$ = 279.95/0.35304 = 792.97 psi

Combined Stress on the lower fiber σ_{UFLF} = -792.97psi + 3098.94 psi = 2305.97 psi

Combined Stress on the upper fiber σ_{UFUF} = 792.97 + 3421.845 = 4214.815 psi

Secondary Bending Stresses on Lower Flange:

$SectionModulus(Z)$ = I/c(Lower fiber) = 0.4413/1.25 $= 0.35304$

$SectionModulus(Z)$ = I/y(Upper fiber) = 0.4413/1.25 $= 0.35304$

Table 3.9 Calculation of secondary bending stresses of lower flange

$\sigma_{b_{LFLF}}$	Lower flange bending stress on lower fiber	792.97psi
$\sigma_{b_{LFUF}}$	Lower flange bending stress on upper fiber	-792.97psi
σ_{LFLF}	Combined stress on lower flange lower fiber	-3213.93psi
σ_{LFUF}	Combined stress on lower flange upper fiber	-5122.25psi

Bending Stress on lower fiber $\sigma_{b_{LFLF}}$ = 279.95/0.35304 = 792.97 psi

Bending Stress on upper fiber $\sigma_{b_{LFUF}}$ = 279.95/0.35304 = -792.97 psi

Combined Stress on the lower fiber σ_{LFLF} = -4006.9 + 792.97 = -3213.93 psi

Combined Stress on the upper fiber σ_{LFUF} = -4329.805 - 792.97 = -5122.77 psi

Vertical Stiffener Strength: Column load in stiffener is given by

$$F_{stiff} = -V_t \frac{d}{h} \tan\alpha = -322.37 * 15.5 * tan(41.7)/19 = -234.3lb$$

Slenderness ratio S_r = length of the column/radius of gyration of the section = l/k

Radius of gyration = 0.267, S_r = 19/0.267 = 71.16

According to the Euler-Johnson theory, if($S_r <$ (l/k_1)) then,

$$\sigma_c = S_y - \frac{S_y^2 S_r^2}{4\pi^2}\frac{1}{E}$$

where l/k_1 = $\sqrt{2\pi^2 E}/S_y \Rightarrow$ l/k_1 = 157.08, S_y = 24000 psi

σ_c = 21537.3 psi

Stiffener strength = $\sigma_c * A_s$ = 4953.58 lb

The column load being only 234.3 lb, this is an over design and can be redesigned to save further weight.

Weight Savings:

Weight of the existing Back Panel = D(t_{old}*w*l + A*l +A*l)= 39.39 lb

Weight according to the new design = D(t_{new}*w*l + A*l*2 + A_s*l_s*3) = 23.55 lb

Total weight savings = 15.84 lb

Table 3.10 Calculation of weight savings

t_{old}	Thickness of the existing panel	0.082 in
t_{new}	Thickness of the new panel	0.02in
w	Width of the panel	16.5in
l	Length of the panel	63in
A	Area of cross-section of upper and lower flanges	0.3985 in^2
A_s	Area of stiffener	0.23in^2
l_s	Length of the vertical stiffener	19in
D	Density of the material	0.28lb/in^3

CHAPTER IV

CONCLUSIONS

As the need arises for stronger, lighter, and environmentally safe vehicles, various design ideas and newer materials are constantly explored. The original material, mild steel, is the material of choice for the new design due to the following reasons:

- reduction in the total structural weight with the new design
- retention of the structural stability
- decrease in the overall material cost
- fuel-savings because of light weight

In the current design, the theory of semi-tension fields has been applied, which is a post buckling phenomenon in which the web continues to carry the load after buckling. The existing back panel of the truck is replaced by a flat sheet thin web supported by vertical stiffeners to allow semi-tension field action. Web is also supported by upper and lower flanges in the form of beams.

A finite element analysis of the newly designed back panel was performed using IDEAS Master series 8 to calculate the maximum load that the back panel can carry. The design load has been determined to be 427 lb. Based on the value of the design load, optimum value of thickness was calculated. Weight savings obtained in the back panel

as a result of the redesign are estimated to be 15.84 lb, which is about 40current weight. Strength analysis of the web had the following results:

- Total shear strength of the panel = 4000.365 lb
- Resistance carried by web in pure shear = 99.495 lb (2.5%)
- Resistance carried by web in tension field = 3852.74 lb (96.3%)
- Remaining 1.2% is carried by the flanges

Strength analysis of the flanges can be summarized as:

- Upper Flange: Stress on the lower fiber = 2305.97 psi
  Stress on the upper fiber = 4212.815 psi
- Lower Flange: Stress on the lower fiber = -3213.93 psi
  Stress on the upper fiber = -5120.25 psi

Tensile and Compressive yield stresses of mild steel being 24000 psi, the upper and lower flanges with the failing stresses around 5000 psi are in a comfortable region with respect to factor of safety.

Strength analysis of the vertical stiffener: The column load that the stiffener is subjected is equal to -234.3 lb. The total strength of the vertical stiffener being 4953.58 lb. The stiffener is far from failing and can be redesigned to save more weight.

Redesign of the back panel by applying the semi-tension field theory proves to be advantageous in perspective of the weight savings as well as the factors of safety. The corresponding analytical results support this argument. This work can be further extended by applying semi-tension fields theory to other parts of the truck to include all the closures. Also, a variety of other new materials with better properties may be applied in order to

further contribute to the overall weight reduction of the vehicle. The theory can be further extended to other types of light truck designs.

REFERENCES

[1] Bruhn E F, *Analysis And Design of Flight Vehicle Structures*, Jacobs Publishing, Inc., 1973.

[2] David J Peery, *Aircraft Structures*, McGraw Hill Book Company, Inc., 1950.

[3] Herbert Wagner, *Flat Sheet Metal Girders With Very Thin Metal Web - Parts I, II, and III*, Tech. Rep. NACA TM 604, 605, 606, National Advisory Committee For Aeronautics, 1931.

[4] Hiroyuki Yamashita and Masakazu Hirano, *Research on the Application of Aluminum Door Beams for Automobiles*, Tech. Rep. 980454, Society of Automotive Engineers, Inc., 1998.

[5] IMPACT Report Validates Steels Long-term future as Material of Choice For Vehicles, "American Iron and Steel Institute," 2001, http://www.steel.org/autosteel/press_room/2001_impact.htm Last Accessed: Aug 20, 2002.

[6] Improved Materials And Powertrain Architectures for 21st Century Trucks, "U.S. Army TACOM National Automotive Center," 1999, http://www.tacom.army.mil/tardec/nac/projects/fordimpact_web.pdf Last Accessed: Aug 20, 2002.

[7] Less Mass from New Materials, "Daniel J Holt, Society of Automotive Engineers," 2002, http://www.sts.sae.org/servicetech/july-2002/less-mass.pdf Last Accessed: Aug 30, 2002.

[8] Lightweight Materials Challenges, "USCAR," 2002, http://www.uscar.org/pngv/techtms/roadmap.htm Last Accessed: Aug 1, 2002.

[9] Oak Ridge National Laboratory, "Lightweight Materials Program," 1999, http://www.ornl.gov/lightmat/Lightweight.html Last Accessed: July 10, 2002.

[10] Paul Kuhn and James P Peterson and L Ross Levin, *A Summary of Diagonal Tension*, Tech. Rep. 2661, National Advisory Committee For Aeronautics, 1952.

[11] PNGV Archives, "U.S. Department of Commerce, Technology Administration," 2002, http://www.ta.doc.gov/pngv/ Last Accessed: Aug 1, 2002.

[12] Steel vs. Light Metals in Automotive Weight Reduction, "Scott Ryan, Cambridge Scientific Abstracts," 1999, http://www.csa.com/hottopics/metals/overview.html Last Accessed: Aug 10, 2002.

[13] Study of Deformation Behavior of Lightweight Steel Structures Under Impact Loading, "U.S. Department of Energy," 2002, http://www.oit.doe.gov/steel/factsheets/lightweight.pdf Last Accessed: Aug 10, 2002.

[14] Trends in weight reduction technology (Kobe Steel), "Kobe Steel Company," 1993, http://www.cs.arizona.edu/japan/www/atip/public/atip.reports.93/weight.93.html Last Accessed: Aug 20, 2002.

[15] Ultra Light Steel Auto Body, "ULSAB," 2002, http://www.ulsab.org Last Accessed: Aug 10, 2002.

APPENDIX

REDESIGN OF AUTOMOBILE DOOR BEAMS

USING ALUMINUM EXTRUSIONS

This chapter reviews previous work done by [4] in order to analyze various factors in the redesign of door beams using aluminum extrusions, which provide the advantages of possessing the same bending strength and energy absorption characteristics as that of high tensile strength steel designs. The study mainly focuses on the redesign technique used to achieve weight reduction in vehicle components. This study has been conducted as part of the literature survey on automobile weight reduction.

The study includes discussion about the effects of varying cross-section and type of alloy used on the performance of the aluminum extrusions. The door beam is a small part used inside the door to prevent the door from being damaged and also to reduce the effect of shock due to collision. Properties such as maximum strength and absorbed energy were determined by the authors, using an approach based upon the three point bending of a beam simply supported at its both ends. Although, the door beam is very small, it is still expected to have high rigidity and strength. Therefore, the possibility of aluminum extrusions, whose cross-section can be varied, is explored for suitability as door beams. The objective of this paper was to show that aluminum extrusions have the desired properties of high tensile strength steel in addition to the advantages aluminum extrusions can offer such as reduced weight, versatility of cross-sections.

As an initial step towards the development of aluminum door beams with the same characteristics as that of the beam made of high strength steel pipe with an outer diameter of 31.5 mm and a wall thickness of 2mm, authors concluded that aluminum alloys with tensile strength at least 400 N/mm2 are needed to reduce weight and also have the same

bending strength as that of steel pipe . Alloys were researched for both the characteristics of strength and extrudability. An alloy Z6W was found suitable for this application.

Table A.1 Typical mechanical properties and possibility of hollow extrusion

Material	TS (N/mm^2)	YS (N/mm^2)	$\delta(\%)$	Extrudability
A7075S-T6	529	461	14	Poor
A7N01S-T6	363	294	15	Excellent
Z6W-T5	480	420	14	Excellent
1470N steel	1529	1029	10	-

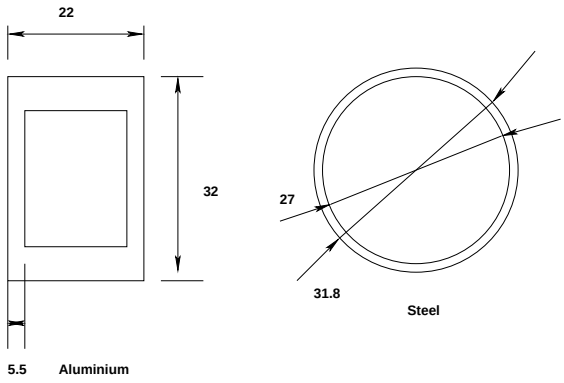

Figure A.1 Cross-sections of Aluminum box section and steel pipe.

In this problem, hollow box section is chosen as the initial cross-section. Table Table A.1 shows that even the high strength aluminum alloys have only half the yield strength and one third tensile strength of high strength steel. Therefore, it becomes necessary to design a cross-section which should be able to support aluminum extrusions and prove fa-

vorable when compared to high strength steel. Hence hollow box section is chosen as the basic section and it is worked on further in this paper, to design an optimum cross-section.

The effects of following factors of the box section on the performance of aluminum extrusions have been studied by doing relevant finite element analyses.

- Wall thickness of the flange and web
- Position of the web
- corner radius

From the theory of bending, bending strength is proportional to the yield strength times section modulus of that particular cross-section. It is observed that moving material away from neutral axis increases the section modulus. The cross-section is investigated for optimum wall thickness of the flange and web. Box section with a constant height of 32mm with varying thickness of flange tf, thickness of web t_w and flange width L was used. A graph is plotted for unit weight versus the width of the flange for different values of flange thickness and web thickness. Appropriate wall thickness and width of the flange are determined using the graph.

It is known that section modulus is independent of the position of the web. Therefore, maximum bending strength is the same even when the web position is changed. Authors have tried to investigate using three point bending test for the five different cross-sections. The author has validated those results by performing a FEM analysis. A graph is plotted between web position and maximum bending strength. This graph shows that maximum bending strength obtained through FEM changes with web position though the

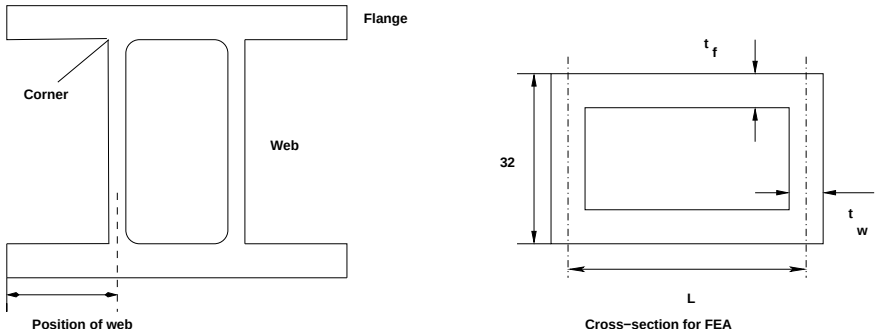

Figure A.2 Box cross-section.

section modulus is still the same. Hence optimum web position can be determined from the graph. A sample calculation is shown below:

$$\text{Bending Stress obtained from IDEAS} \quad = \quad 31371\text{lb-in}$$

Converting this into kN to match the graph plotted by the authors(as shown in figure A.5),

$$\begin{aligned}
\text{Tensile Strength of the material} &= (480N/mm^2) * 145 \\
&= 69600 * 1000psi \\
\text{Ratio} &= 69600000/31371 \\
&= 2.22lbf \\
\text{Bending strength} &= 2.22 * 4.448 * 1000 \\
&= 9.875kN
\end{aligned}$$

Similarly, bending stress obtained for the ratio,

$$\begin{aligned}
B/L1 &= 1 \\
&= 29321.55lb - in. \quad \text{(From FEA as shown in figure A.3)}
\end{aligned}$$

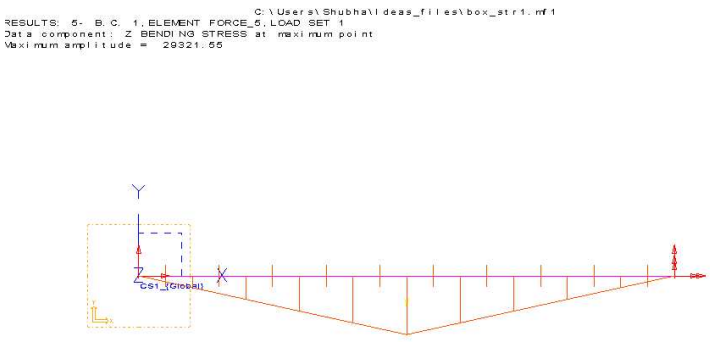

Figure A.3 Maximum bending strength Calculation.

Following the same procedure described above

$$\text{Ratio of tensile strength and bending stress} = 69600000/29321.55$$

$$= 2.3737.$$

$$\text{Therefore, Bending strength} = 10.55kN$$

Hand calculation:

$$\text{Bending stress} = \text{(Max. bending moment)/(Section modulus)} \quad \text{(A.1)}$$

$$\text{Section modulus} = \text{I/c} \quad \text{(A.2)}$$

Where:

$I =$ Moment of inertia $= 0.16917in$

$c =$ Distance from the neutral axis $= 0.63in$

$z = 0.16917/.63 = 0.2686$

Bending stress $= 8250/.2686 = 30714.82psi$

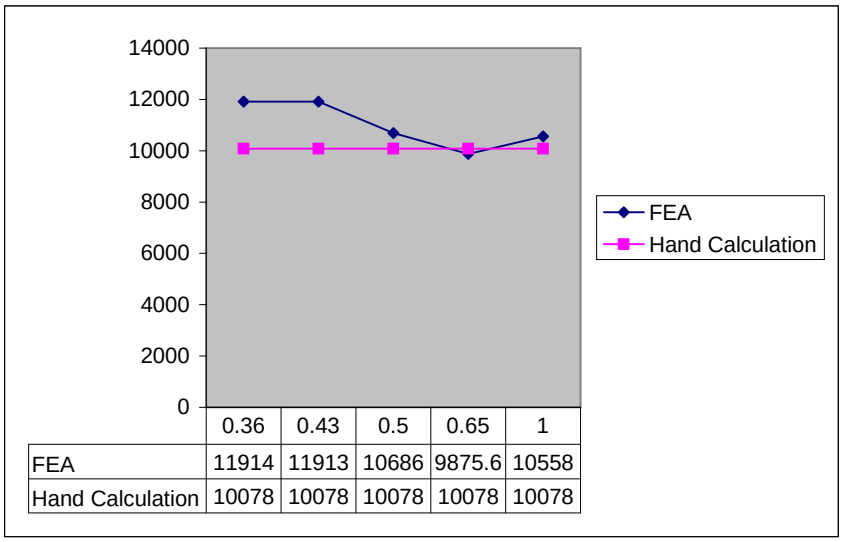

	0.36	0.43	0.5	0.65	1
FEA	11914	11913	10686	9875.6	10558
Hand Calculation	10078	10078	10078	10078	10078

Figure A.4 Graph showing Bending Strength versus web position.

(see figure A.5)

Following the above procedure for conversion into bending strength = 10.08kN Corner radius: Maximum bending strength was calculated from FEM analyses for the following modified cross-sections.

- Basic: $t_w = 1.9$ R = 1
- With different corner radius (R = 4)
- With different $t_w(= 2.2), R = 4$

Bending strength ratio:

$=$ (Bending stress of basic)/(Bending stress of modified section) (A.3)

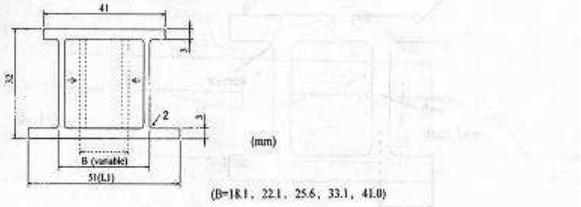

Fig.7 Cross-section which B varied

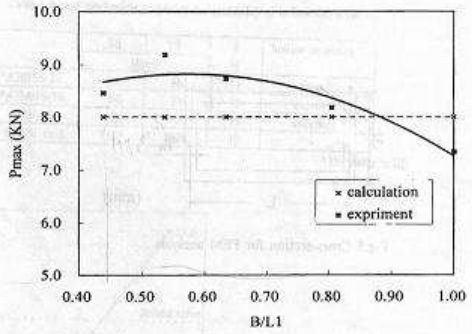

Fig.8 Relation with web position and maximum bending strength

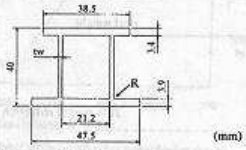

(a):Basic (tw=1.9, R=1)
(b):With different corner radius (tw=1.9, R=4)
(c):With different tw (tw=2.2, R=4)

Fig.9 Cross-section to investigate the corner

Table 2 bending properties of door beam on Fig.9

	weight	maximum strength	energy absorption
basic section	1.00	1.00	1.00
modification of corner	1.05	1.04	1.29
addition web thickness	1.09	1.07	1.73

(Ratio for basic section)

Figure A.5 Results from the Paper.

Therefore, ratio $= 1.04$

Modified corner case $= 7791.7/7453.902$

Ratio (modified web thickness) $= 7791.7/7312.705$

$= 1.07$

Table A.2 Values of strength for modified corner radius and web thickness

	Weight	Maximum strength
Basic section	1.00	1.00
Modification of corner	1.05	1.04
Addition web thickness	1.09	1.07

Authors have concluded based on the above results that aluminum door beams can be successfully developed that have a maximum bending strength equivalent to that of the high strength steel door beam and achieve a weight savings of 22 $\%$ over the steel beams. But the conclusion is not entirely right. Evidently, results remain valid for the specific cross-sections(steel pipe and aluminum box)chosen. Alternatively, steel pipe can be hydroformed to a box cross-section and the values can be recalculated. The new dimensions of the hydroformed steel cross-section can be calculated as follows:

Outer diameter of the steel pipe d_o = 31.8 mm

Inner diameter of the steel pipe di = 27 mm

Moment of inertia of outer circle $I_o = \pi * d_o^4/64$ = 5.02 * 10^4 mm^4

Moment of inertia of inner circle $I_i = \pi * d_i^4/64$ = 2.61 * 10^4 mm^4

Moment of inertia of the steel pipe cross-section $I_{circle} = I_o - I_i$ = 2.41 * 10^4 mm^4

Area of the pipe cross-section $A_{circle} = \pi(d_o^2 - d_i^2)/4$ = 221.67 mm^2

Thickness of the hydroformed section t = $\frac{d_o - di}{2}$ = 2.4 mm

Height of the hydroformed section h = 32 mm

Width of the hydroformed section b = $(A_{circle} + 4t^2 - 2ht)/2t$ = 18.9814 mm

Table A.3 Dimensions of the steel pipe and hydroformed section

d_o, di	Outer and Inner diameters of steel pipe	31.8, 27 mm
w	Width of the hydroformed section	18.9814 mm
h	Height of the hydroformed section	32 mm
t	Thickness of the hydroformed section	2.4 mm

Moment of inertia of the hydroformed rectangular section(outer)I_{rectO} = $bh^3/12$ = 5.183* $10^4 mm^4$

Inner dimensions of the rectangular section can be calculated as: height h1 = h - 2t = 27.2 mm

width b1 = b - 2t = 14.18 mm

Moment of inertia of the inner rectangular section I_{rectI} = $b1h1^3/12$ = 2.378 * $10^4 mm^4$

Ratio of moments of inertia of circle to rectangular ratio = I_{circle}/I_{rect} = 0.8595

It is seen that the hydroformed section has higher moment of inertia than the original pipe design. Therefore dimensions are recalculated based on the ratio so that the new section and old section do not differ significantly.

Modified area of the rectangular section A_r = A_{circle} * ratio = 190.5336

Similarly, modified thickness t1 = t*ratio/1.038 = 1.9874 mm

Therefore, the new height h1 = h - 2t1 = 28.0253 mm

New width b1 = b - 2t1 = 15.0067 mm

Moment of Inertia of the rectangular section (modified dimensions) I_{rect1i} = $b1 * h1^3/12$ = 2.7527 *10^4

Table A.4 Modified Dimensions of the hydroformed section

w1	New Width of the hydroformed section	15.0067 mm
h1	New Height of the hydroformed section	28.0253 mm
t1	New Thickness of the hydroformed section	1.9874 mm

Moment of Inertia of the total section I_{rect1} = $I_{rectO} - Irect1i$ = 2.4305 *10^4

Increase in Inertia(pipe-rectangular) = I_{rect1}/I_{circle} = 1.0085

Area of cross-section of the modified section A1 = bh - b1h1 = 186.8367

Weight of the modified section = original weight of the pipe* A1/A_{circle} = 1.48*186.8387/221.67 = 1.2474 kg/m

New Bending strength = original bending strength * I_{rect1}/I_{circle} = 11.8956 kN

Therefore, the hydroformed section of steel has comparable values of bending strength and weight with the aluminum box section.

Table A.5 Results comparison of Aluminum and Steel door beams

Material	Maximum Strength (kN)	Unit Weight (kg/m)
1470N steel	11.8	1.48
Aluminum	11.5	1.16
Hydroformed steel pipe	11.8956	1.2474

Though the calculations and experimental values in the paper are verified to be correct, conclusions made by the authors with respect to achieving weight savings of 22$\%$

when compared to steel designs are not acceptable and has been demonstrated by taking an alternative cross-section of steel section.